Deep Mining 2024 – P Andrieux & D Cumming-Potvin (eds)

doi:10.36487/ACG_repo/2465_49

Three-dimensional modelling of development intersections at the Eleonore mine

Gregory Turfan [a,b,*], Shahé Shnorhokian [a], Hani S Mitri [a], Amanda Conley [b]

[a] *Department of Mining and Materials Engineering, McGill University, Canada*

[b] *Newmont Corporation, Canada*

Abstract

Several ground control challenges are encountered during the narrow-vein mining of parallel orebodies in a complex geologic environment at the Eleonore mine. Mining-induced seismicity and related rock mechanics instability events often take place at vulnerable locations such as development intersections. Both static and dynamic ground support systems are used to control the effects of these events. The mining sequence followed is usually pyramidal and moves from bottom to top with regional pillars separating the different blocks. Numerical modelling is used to assess the stress redistributions based on the stope sequences being planned.

In this paper a geometrically simplified 3D linear elastic model of the Eleonore mine is constructed for several levels, along with the drift and crosscut systems on L 860, L 830 and L 800. Rock mass properties used as model inputs are obtained from recent laboratory tests and core logs, as well as older studies conducted for the Eleonore mine. Calibration is conducted with boundary stresses being applied to obtain pre-mining magnitudes comparable to those measured in the field. A typical pyramidal sequence is implemented and locations within the development network where potential instability could take place are identified based on σ_1 and brittle shear ratio (BSR) thresholds. Based on these initial results a detailed 3D model is then constructed of potential vulnerable intersections. The outputs from the two models are compared and the impact of mining is assessed with respect to the mode of instability observed at these intersections.

Keywords: *development intersections, mining-induced seismicity, 3D modelling, stope sequences*

1 Introduction

Eleonore is a gold mine located in the James Bay area of northern Quebec. A good portion of the deposit sits beneath the Opinaca reservoir and extends to surface in the Roberto area. It extends 1.9 km along the strike and is at least 1,400 m in depth. The 'crescent' or, more locally, 'W' shape of its mineralisation consists of numerous thin gold zones ore lenses, the most important being the 5050 and 6000. These lenses are generally 5 to 6 m in thickness but can vary locally from 2 to more than 20 m. The host rock of the mineralised zones is composed of a slightly foliated and bedded greywacke that is traversed occasionally by pegmatite dykes, and quartz veins and veinlets. Other lithological units include conglomerates, schist, diorite intrusions and diabase dykes.

Another particularity of the Eleonore mine is its complex regional fault system, which consists of many sub-horizontal units mostly located in the upper portion of the mine (0–800 m), and northwest-southeast striking sub-vertical faults which are mostly visible and reactive in the lower part of the mine (below 800 m). The sub-horizontal faults normally consist of 1–3 m-thick zones of highly fractured ground and/or gouge, and most of these are also water-bearing structures. The sub-vertical faults form anastomosing fracture systems going up to 5 m in thickness and are characterised by dense breccia veins. In some areas they are observed

* Corresponding author. Email address: gregory.turfan@mail.mcgill.ca

to display high and dense foliation with high contents of biotite. The main sub-vertical faults also typically show one distinguished joint filled with a thin gouge layer. As described by Terrane (2019), the latter are brittle reactivations of older ductile shear zones and are attributed to a sinistral strike-slip faulting event associated with the latest regional deformation event. Many seismic events occur around these faults and the nodal planes associated with them do not correlate perfectly with the strike and dip of the fault zones themselves, meaning that there are different joints or fractures involved in their rupture process.

The Eleonore mine is divided into different horizons, with each counting around six levels separated by 30 m. Mining is conducted distinctly in each horizon using a bottom-up pyramidal sequence and a narrow-vein sub-level stoping method. These bottom-up sequences inevitably create sill pillars in the upper part of the horizons, squeezing stress between the stopes of the ongoing sequence and the already mined stopes of the superior horizon. These high induced stresses, combined with the complex fault system and adverse lithologies, create an optimal environment for rock instability and rockbursting conditions.

The fifth horizon (H5) that extends from level 980 to 830 has so far been the most geotechnically difficult horizon to extract at Eleonore. Mining is still ongoing there and many stopes are still to be taken in the upper part of the horizon. However, drifts on levels 830 and 860 specifically have degraded very fast and were already displaying significant deformation even when the extraction ratio was still relatively small. The static depths of failure were enhanced drastically by the intense and constant seismicity that occurred on these levels. Multiple time-consuming and robust rehabilitations, including the installation of steel arches and cable bolts, have been conducted and are still being carried out to keep the area stable and secure for mining.

1.1 Brittle rock behaviour

Brittle rocks like the ones at Eleonore behave in a particular manner when loaded. The failure is preceded by a damage process which initiates well before the peak strength of the rock is reached. In fact, Bieniawski (1967) showed that in the laboratory, for massive to moderately jointed rock masses under unconfined compression conditions (UCS tests), cracks start initiating at approximately 30 to 50% of the peak UCS value. At 70 to 80%, the author showed that the yield strength of the rock is reached, and at that point cracks were observed to grow in an unstable manner (Bewick et al. 2019). Failure occurred after some time if the stresses were maintained. However, Martin (1993) showed that at low confining stresses (e.g. close to the excavation surface) in the field, the rock mass strength or yield was often 30 to 50% of the UCS, which coincided with the crack initiation threshold in the laboratory (Bewick et al. 2019). Once this threshold is reached, brittle failure occurs by tensile spalling, which consists of cracks parallel to the surface of the excavation in the back. Cook (1983) referred to them as ‘cleavage fractures’ and stated that they tend to follow the direction of the maximum principal stress. They consist of tensile cracks and their extensional movement is directed towards the excavation opening. In addition to spalling, slip along cracks or fractures of joints can also occur. As the load approaches the peak strength of the rock, Griffith-like propagation of the cracks occurs (Kaiser & Cai 2013). The rock mass slowly fragments and disintegrates itself, with rock bridges being broken as pre-existing microfissures grow and coalesce, and critically oriented discontinuities are sheared and opened. In other words, an almost continuum rock mass medium, often with non-persistent joints, is transformed into a ‘loose’, cohesionless discontinuum with mostly continuous and open fractures (Kaiser & Cai 2013). This type of brittle failure occurs in the low confinement range and close to the surface of excavations. In high confinement ranges, the length of the tensile cracks is enormously reduced. This was confirmed by many authors, such as Germanovich & Dyskin (1988), Martin (1997), Cai et al. (1998) and others who conducted theoretical studies on closed cracks.

However, Cai & Kaiser (2014) conducted a study using modelling and real field data from the Mine-by tunnel at the Underground Research Laboratory in Canada. In their article they debate the fact that the in situ (in-field) strength of massive rocks might be much higher than 0.4 ± 0.1 UCS, which is the widely accepted failure criterion for brittle rocks. Instead of modelling a perfectly rounded drift they modelled the Mine-by tunnel with the exact shape it had, meaning that they included all angular parts the boundary of an excavation typically has. All of these irregularities in the boundary caused stress raisers and showed much higher stress magnitudes around the excavations. By comparing these results to the real in-field depth of

failure they showed that, with the true 'as-built' excavation boundary, the 'actual' rock strength is much higher (around 0.8 UCS). As they explained, it was still possible and correct to use a 0.4 UCS 'apparent' rock strength when modelling only when simplified excavation boundaries (smooth circular arch without irregularities) were used throughout the model. They stated that these were not the actual strengths and that they should not be used when inferring rock properties in other realistic geometric conditions or when designing pillars (Cai & Kaiser 2014).

Before a tunnel is excavated, the depth of fractured and unstable rock can be estimated using the stress level ratio. The stress level (SL) considers the confinement, i.e. σ_3, and is defined as $(3\sigma_1–\sigma_3)/UCS$, where the term $(3\sigma_1–\sigma_3)$ is the maximum tangential stress at the wall of a circular opening in elastic ground conditions (Kaiser & Cai 2013). At low stresses, when the maximum tangential stress is around 25% of the UCS, the back (or wall) will be stable under static conditions and damage can only be inflicted by the addition of high dynamic stresses, i.e. a large seismic event. At intermediate stresses when SL > 0.3, stress-driven failures slowly begin to take place. 'Loose ground' starts to form (Kaiser & Cai 2013) and stress-induced fractures propagate from stress raisers at the corners of the excavations towards the middle of the excavation, forming semicircular fracture patterns (typically called 'onion skinning') around the opening (Kaiser et al. 1996). This tension fracture zone is called 'baggage', and in practice is created by stable failure processes in which the stored strain energy in the rock mass is consumed during the fracture and deformation process (Kaiser et al. 1996). The thickness of this fractured zone is defined as 'the depth to which the rock mass, if left unsupported, would disintegrate to such an extent that its coherence is completely disrupted and the rock would fall apart under gravity alone' (Kaiser et al. 1996). When the static critical SL is reached, which is normally around 0.42 for massive rock (Kaiser & Cai 2013), the opening becomes meta-stable. Minor strainbursting and popping ground should be expected and, at that point, even a small perturbation of the stress field will trigger failure. Deepening of the zones of failed rock is now possible due to dynamic stress increments from a seismic event nearby. At very high stresses, greater than 50% of the UCS or at stress levels higher than 65%, deep-seated stress failure dominates and baggage is directly created at the moment the opening is excavated (Kaiser & Cai 2013; Kaiser et al. 1996). Strainbursts create 'dog-ear shape' failure zones due to the action of dynamic stress pulses and the non-uniform in situ stress field (Kaiser et al. 1996). During these stress-driven failure processes, the rock mass is strained due to high tangential stresses and the originally intact parts are broken into rock blocks and fragments of different sizes. Bulking occurs as a result of the geometric non-fit of these hard rock blocks, and the broken rock can only move in the radial direction into the excavation. Bulking is a unidirectional length change (Kaiser & Cai 2013), which is highly dependent on confinement and is much larger near an excavation than when it is confined (Kaiser & Cai 2013). This brittle rock deformation process will load the support components directly (at the plate) or indirectly (inside the rock mass).

1.2 Intersection instability at the Eleonore mine

The complex geology at the Eleonore mine creates ground control challenges. Modelling studies such as those from Garza-Cruz et al. (2019) show that the shearing of Eleonore's sub-horizontal joints due to high stress is one of the main factors for bolt straining inside the rock mass. Bulking is also a result of Eleonore's high stress regime, and reinforcement of the support needs to be made often when bulking loads compromise the mesh and bolt plates. Instability occurrences are particularly observed at H5 horizon, especially on the top levels (such as the 830 and 860). The rock mass on these levels has degraded quickly, displaying a high state of deformation even before stopes nearby were taken. The exact reasons regarding this phenomenon on these levels are still unknown. Large intersections on the 830 and 860 levels have been, and still are, monitored very closely. It is widely known that they are more prone to failure than typical drifts because of their large spans, and therefore have high potential for deformation. In addition, they may be vulnerable to seismicity because of their lower confinement, which makes the rock mass at intersections weaker and thus easier to rupture. Hence the ground support at an intersection must be robust enough to prevent large wedges from falling and large volumes of fractured rock from unravelling. These potential instabilities must be controlled and the rock mass tensile load capacity must be preserved by using long, strong and stiff bolts, as well as a tough surface support (Kaiser et al. 1996). Examples of intersection failures are shown in Figure 1.

(a) (b)

Figure 1 Example of intersection failures in mines: (a) Heavily fractured rock; (b) Large blocks

In this paper, 3D numerical modelling is used to simulate multiple intersections on three levels in the upper section of H5 at the Eleonore mine. First a geometrically simplified model is used to assess the effect of excavating the developments and stopes on potential instability at the intersections. In the second phase, intersections observed to be vulnerable to high compressional or shear stresses are replicated in a separate model, using their actual geometries and a higher mesh density for a more detailed evaluation.

2 Numerical modelling methodology

Two different models were constructed in the finite difference code FLAC3D (ITASCA 2019) to assess potential instabilities at development intersections at the Eleonore mine. For both models, stopes from the central pyramid going from level 920 to 740 were incorporated and excavated using the actual as-mined sequence. The stopes are not the focus of this study but, as they generate most of the induced stresses on the development drifts, they were modelled to obtain a more realistic assessment of the situation. In the first case a geometrically simplified version of the 5050 and 6000 lenses — as well as the main drift system to their east — was constructed for levels 800, 830 and 860. Additional levels were added to the top and bottom to allow the areas of interest to be at a distance from the model boundaries. The final dimensions were 1,350 m in the north–south direction, 700 m in the east–west direction and 510 m in depth. Rock mass properties from a previous report (Golder Associates 2009) were used as input parameters for the model, and calibration was conducted using boundary tractions such that stress magnitudes on levels 645, 765 and 885 matched those proposed by previous studies (Bouzeran et al. 2018; Corthésy & Leite 2017; Yong 2014). All drifts and crosscut systems on levels 800, 830 and 860 were excavated simultaneously in the calibrated model. This was followed by stope sequence extraction on levels 800 and 770, and then with mining on levels 920, 890, 860 and 830 below. Mining and backfilling were simulated, with three stopes being extracted in each stage. Due to the occurrence of frequent microseismic events at the mine, the maximum principal stress (σ_1) and the brittle shear ratio (BSR) were monitored during the various stages of excavation and ore extraction to assess the potential for instability. Figure 2 presents an isometric view of the developments on the three levels in the geometrically simplified model, whereas Figure 3 illustrates the detailed model.

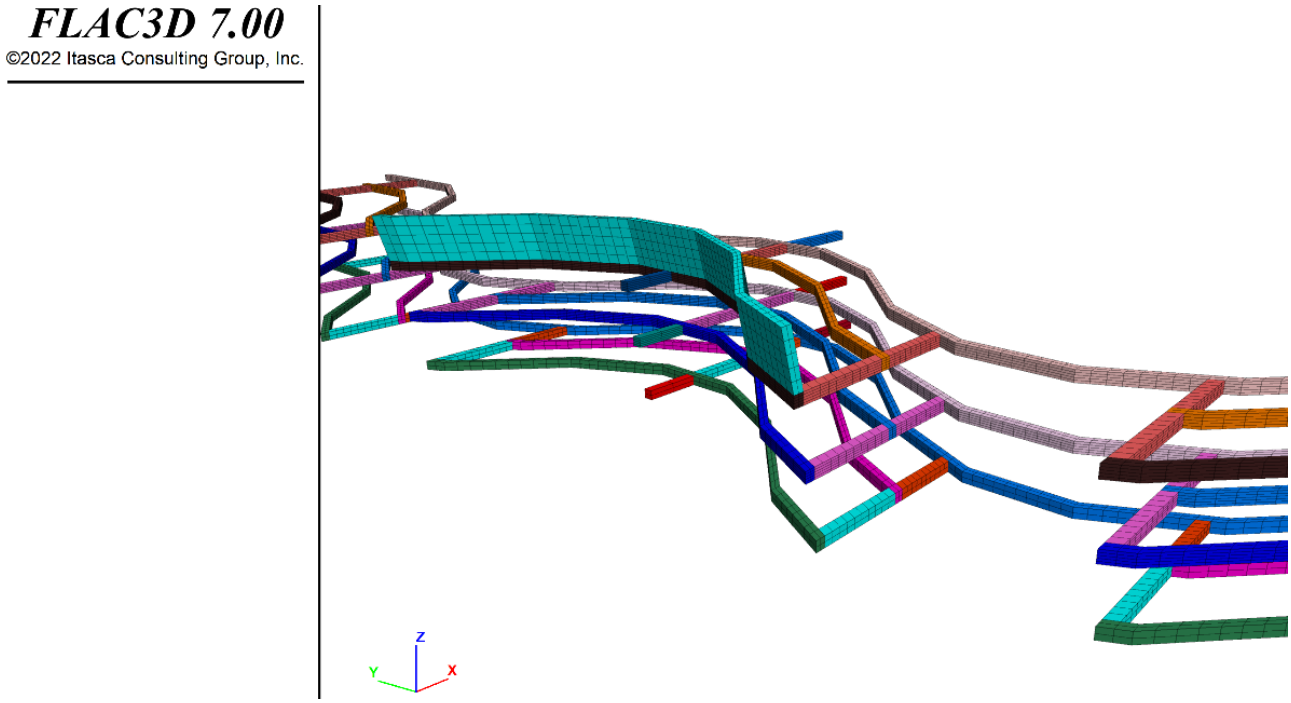

Figure 2 Isometric view of developments on three levels and stopes above them in the geometrically simplified model

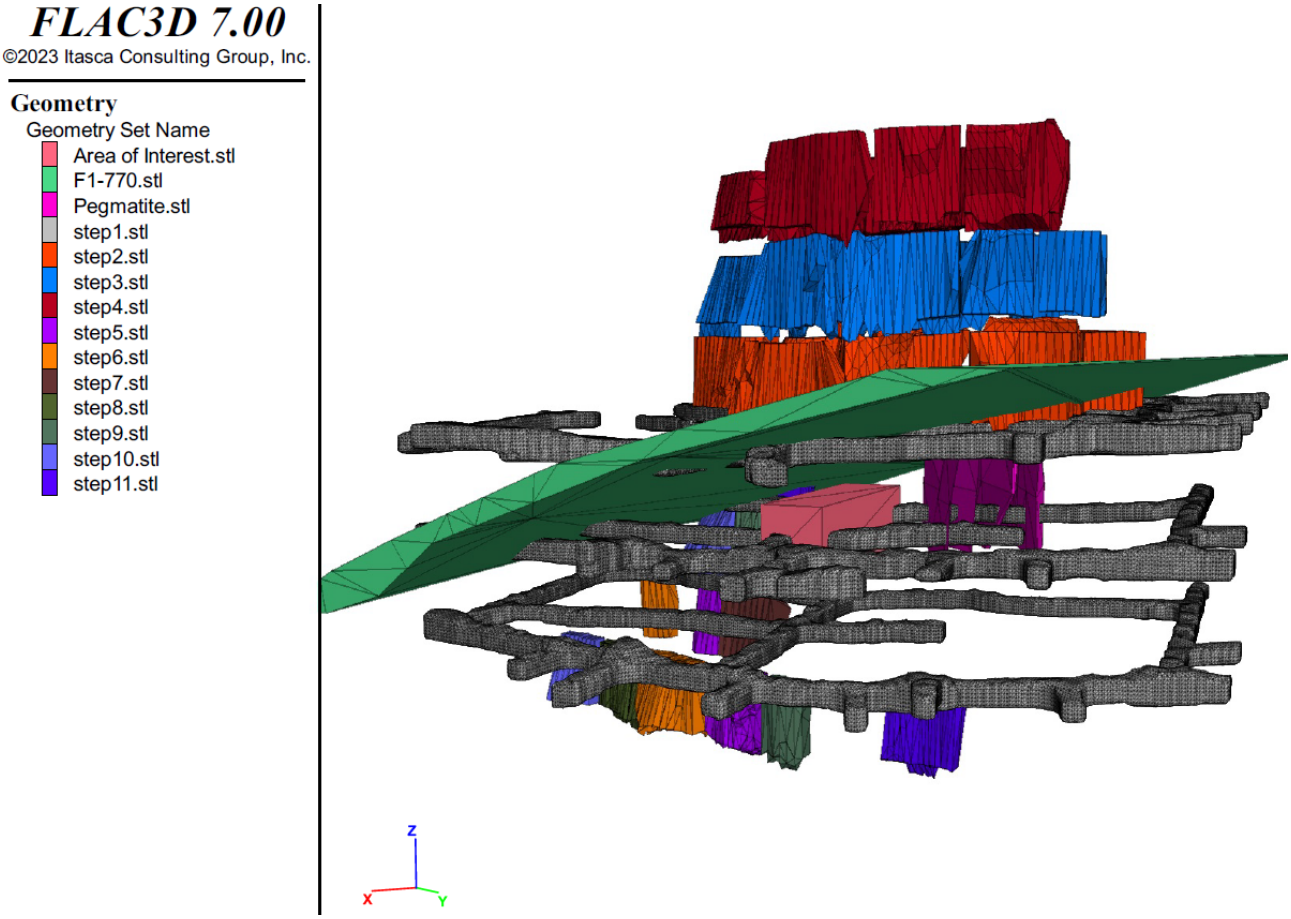

Figure 3 Isometric view of developments on three levels and stopes above them in the detailed model

Based on results obtained from the simplified model, a second one was constructed using a combination of StopeX (Vakili et al. 2020) and FLAC3D. StopeX is a digital tool, developed specifically for use with FLAC3D, which reduces the time required for complex geometry construction. It converts geologic and geometric data in CAD software into a model that can be simulated in FLAC3D, and uses an improved unified constitutive model (IUCM) (Vakili 2016) for elasto-plastic strain-softening analysis as the basis for calculating stress and displacement magnitudes. The second model was constructed based on the factual geometry files from the mine for intersections that were identified in the initial geometrically simplified version as being vulnerable to potential instabilities. Several advantages were associated with this second model, including the focus on a smaller region, constructing it with a more densified mesh, and being based on the actual – and not simplified – geometry. The combined approach of using a geometrically simplified general model followed by a more detailed one allows for multiple sequences to be assessed in the former, which then indicate areas of potential interest. The latter would then be constructed with the aid of StopeX and provide detailed information regarding the form and volume of instability. Both models were run in linear elastic mode to maximise induced stresses and present a conservative assessment of burst-related instability. The detailed model was also run in elasto-plastic strain-softening mode using the IUCM to assess the differences in results. Since compressional and shear types of failure were being assessed with respect to rockbursting, and because the linear elastic model resulted in more areas being susceptible to them (more conservative), it was selected for a comparison with the geometrically simplified model. Figure 3 presents an isometric view of the developments on the levels, stopes and geologic structures in the detailed model.

The comparison between the two models forms the basis of this study, where the objective is to determine whether a geometrically simplified model — easier and faster to construct and to run – could help engineers to first identify areas of high risk. Following the initial findings a detailed model would be necessary only for these specific areas, and therefore the time needed for model construction and computation is reduced. Since most of the instabilities at the Eleonore mine have taken place at the intersections, the focus of this study will be on the induced stress at the boundaries of the developments.

2.1 Model input parameters

Rock and rock mass properties used as model input parameters were derived from laboratory testing and core logging records. In the geometrically simplified model, the wacke and orebody were the only geologic formations replicated, while the pegmatite and the F1-770 fault were added in the second factual model. Calibration of both models was conducted based on previous reports of in situ stress measurements (Bouzeran et al. 2018; Corthésy & Leite 2017; Yong 2014). In addition, the generated in situ stresses prior to development excavation and mining were compared between the two models for further validation. Table 1 presents the input rock and rock mass parameters used for both models, and upon which the instability analysis was conducted.

Table 1 Rock mass properties used for model input and instability analysis

Geologic unit	Density (kg/m^3)	E_i (GPa)	ν	UCS_i (MPa)	RMR	E_{rm} (MPa)	K (MPa)	G (MPa)
Wacke	2,750	39.05	0.14	111	75	28,616	13,248	12,551
Pegmatite	2,500	59.00	0.22	97	70	43,236	25,700	17,700
Orebody	2,790	46.26	0.13	196	78	36,327	16,363	16,074

In the geometrically simplified model, the bottom was fixed and tractions were applied to the boundaries until directional stresses were within 5 MPa of readings on 885 level, based on in situ measurements and formulas from previous reports (Bouzeran et al. 2018; Corthésy & Leite 2017; Yong 2014), as presented in Table 2 below. In the detailed model, values using the same formulas were input into StopeX and the stresses were generated based on the traditional FLAC3D approach of initialising them.

Table 2 In situ stress regime magnitudes and trends used for model calibration

Stress	Magnitude (MPa)*	Trend (°)	Plunge (°)
σ_3	27.5 × z	0	90
σ_2	27.5 × z	153	0
σ_1	19 + 27.5 × z	63	0

* z = depth in km

2.2 Instability criteria

The selection of instability criteria was made based on the rock mass behaviour at the Eleonore mine. Due to the prevalence of seismic activity and rockbursting events, the two main parameters examined were the σ_1 and the differential stress (σ_1–σ_3). With the former a comparison can be made with the UCS_i of a given geologic formation to assess the potential for compressive failure, especially at the excavation surface where σ_3 is zero. Another criterion is the BSR, which compares the differential stress to the UCS_i of the rock mass. The BSR can be related to the maximum shear stress value since the latter constitutes half the differential stress (σ_1–σ_3). Castro et al. (2012) suggested several ranges of BSR values, which would indicate different levels of rock mass damage and the potential for strainbursting, as presented in Table 3. In this study a BSR of 0.45 was used as a threshold for moderate rock mass damage and an indication of minor strainbursting. As a conservative assessment of instability potential the lower UCS_i value of the wacke was used instead of that of the orebody, which translates into a differential stress of 49.95 MPa and a maximum shear stress of 24.98 MPa. It should be noted that a BSR of 0.7 indicates that major strainbursting would therefore be equivalent to a maximum shear stress of 38.85 MPa.

In addition to the BSR-maximum shear stress criterion, the σ_1/UCS_i ratio was adopted as an indication of crack initiation and crack damage. An average threshold of 0.6 was used, as this is between the crack and damage thresholds (0.4 and 0.8, respectively) proposed by Bieniawski (1967). Naturally the phenomenon would be applicable at the boundaries of developments and would indicate the potential for instability. The expanded surfaces of intersections, combined with the absence of confinement ($\sigma_3 = 0$), means that the ratio would be especially indicative of their vulnerability to compressional failure.

Table 3 Brittle shear ratio ranges for rock mass damage and the potential for strainbursting (Castro et al. 2012)

$(\sigma_1–\sigma_3)/UCS_i$	Rock mass damage	Potential for strainbursting
0.35	No to minor	No
0.35 to 0.40	Minor (e.g. surface spalling)	No
0.45 to 0.6	Moderate (e.g. breakout formation)	Minor
0.6 to 0.7	Moderate to major	Moderate
>0.7	Major	Major

2.3 Mining sequence

In both the geometrically simplified and detailed models the sequence of mining followed was identical. Once the pre-mining stresses were generated during the calibration phase, the first stage comprised the excavation of all developments on all the relevant levels. In the second stage the stopes above the area of interest – level 830 – were mined and backfilled to provide the baseline, after which a pyramidal sequence was implemented from level 920 upward. Three stopes were mined and backfilled at each simulation stage to provide a balance between computation time and model stability. Figure 4 provides a detailed sequence of stoping between these levels at the Eleonore mine.

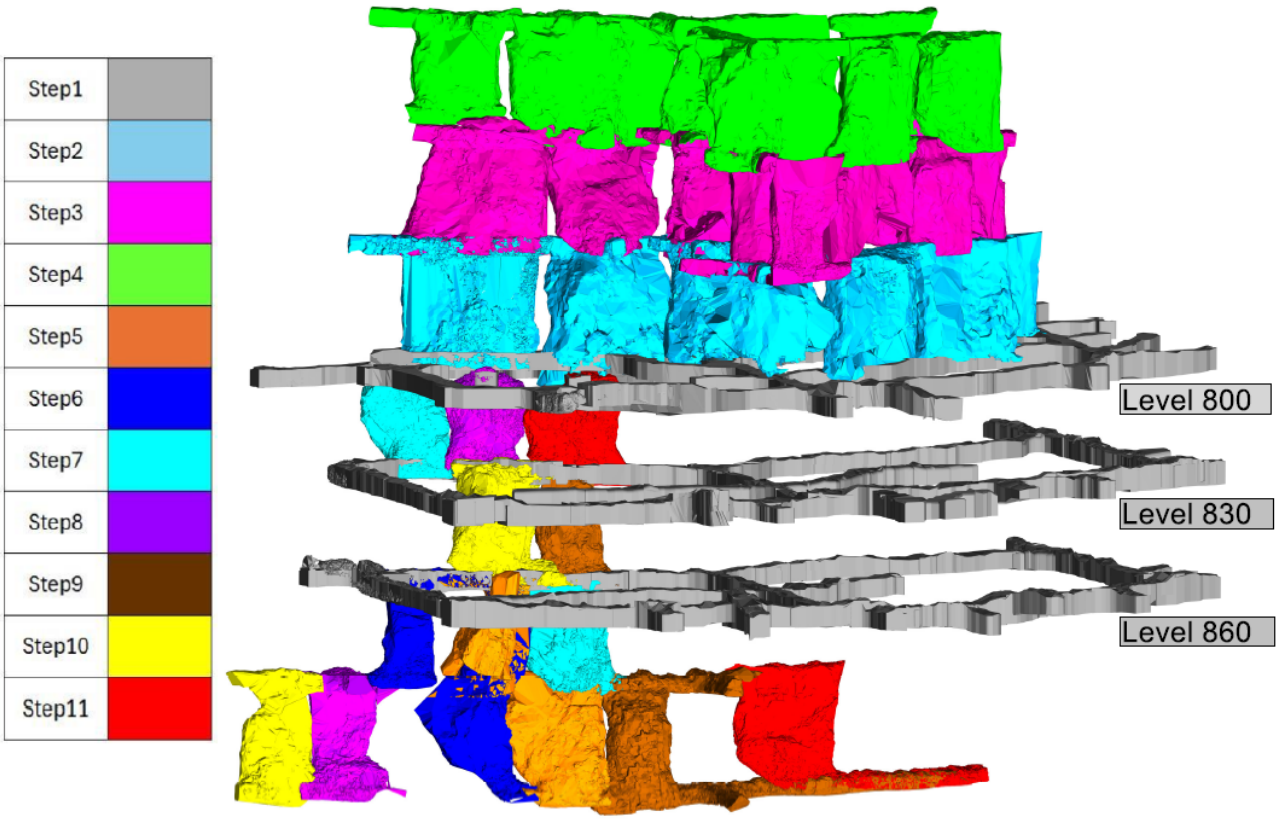

Figure 4 Stope sequencing followed between levels 920 and 740

3 Results and discussion

As indicated in the previous section, two models were constructed for this study. Hence the results obtained from each one will be discussed separately in the sections below. The σ_1 and shear stresses are adopted to evaluate the potential of microseismic activity and rock instability. The former is compared directly to the UCS_i of the geologic units while the latter is back-calculated from a BSR threshold of 0.45 for moderate damage potential and minor strainbursting. With a UCS_i of 111 MPa the wacke requires a differential stress (σ_1–σ_3) of ≈50 MPa for this to occur, which translates into a maximum shear stress value of ≈25 MPa. On the other hand, a σ_1 magnitude of ≈67 MPa would be required for compressional damage to occur in the wacke. The rock mass properties of this geologic unit were selected as the basis for assessment due to their lower instability threshold when compared to those of the orebody. Furthermore, due to the geometrical characteristics of narrow veins, most of the developments are located within the host rock rather than in the orebody.

3.1 Simplified model

Results from the geometrically simplified model indicate that after initial equilibrium is attained and the pre-mining stresses are generated, no significant stress concentrations appear on levels 800, 830 and 860. The highest σ_1 value observed occurs along the straight sections of the W-shaped thin lenses presented in Figure 5, and ranges between 45 and 50 MPa. The same locations also host maximum shear stress concentrations of 12 MPa. For the pre-mining phase, both compressional and shear stress magnitudes are well below the failure criteria of 67 MPa and 25 MPa, respectively, as set above. At stage 1 all the developments on the three levels are excavated in one step, with the σ_1 and maximum shear stress distributions on level 860 presented in Figure 5. It can immediately be observed that all three intersections along the east–west axis carry a slightly higher σ_1 concentration of 49 MPa in their northeast and southwest corners. The east–west crosscuts in the northern, central and southern sections of the lenses all exhibit the same trend. A similar pattern emerges for these intersections when the maximum shear stress is plotted on level 860 where values of 15 MPa are observed. The same trends are present on levels 800 and 830, thus

confirming that all intersections between the north–south drift or undercuts and the east–west crosscuts become vulnerable to elevated σ_1 and maximum shear stress magnitudes after they are excavated.

A major increase in both σ_1 and maximum shear stress occurs at the first stage of stoping on level 800 that commences in the northern part. The westernmost intersection immediately below the extracted stopes exhibits a σ_1 magnitude of 70 MPa, which represents a significant increase from the initial values of 49 MPa observed after development excavation. The maximum shear stress also increases from 15 to 33 MPa, thus breaching the 25 MPa threshold for moderate rock mass damage and minor strainbursting. The magnitudes of σ_1 and maximum shear stress remain stable on the lower levels of 830 and 860 due to their distance from stoping activities above. The same trend is observed at the other intersections on level 800 further to the south, where mining activities have not yet started.

With the completion of mining and backfilling on level 800 an elevated σ_1 magnitude is observed along the eastern boundary of the north–south developments there. Of prime interest for the stability of intersections is the stress concentration at the central crosscut intersection where σ_1 attains 94 MPa. This indicates that the σ_1/UCS_i threshold of 0.6 (67 MPa) has been superseded and compressional failure can take place. In the same stage the maximum shear stress reaches 44 MPa and is therefore above a BSR of 0.7, which indicates major rock mass damage and strainbursting potential. Figure 5 presents the σ_1 and maximum shear stress distributions on level 800 after all stoping is completed above.

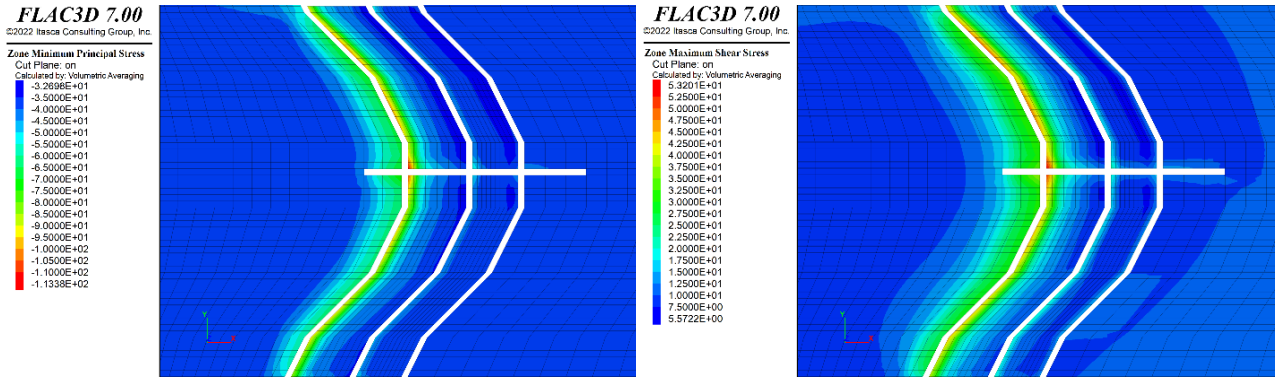

(a) (b)

Figure 5 Geometrically simplified model results after stoping above level 800: (a) σ_1; (b) Maximum shear stress

3.2 Detailed model

For the detailed model, isosurfaces of maximum shear stress and major principal stress were plotted in conjunction with the drift geometries. The isosurfaces were plotted for stages 1, 4 and 11 (see Figure 4 for details). For the σ_1 isosurface, a value of 66.6 MPa was chosen since it resides between the crack (0.4 UCS = 44.4 MPa) and damage (0.8 UCS = 88.8 MPa) thresholds described by Bieniawski (1967). When the three stages are compared, high stresses are observed starting at the boundaries of the intersections and slowly migrating towards their centre (see Figure 6). It is also noted that level 830 is more affected than level 860, which is logical because the former constitutes a sill pillar level. In addition, the west lens (5050) also seems to show a larger volume of high stresses than the east one (6000).

The maximum shear stress seems to behave in the same way as the major principal stress, with isosurfaces becoming very large in the final step (step 11). They are plotted for a value of 25 MPa, which translates to minor potential for strainbursting (see Section 2.2 and Figure 7).

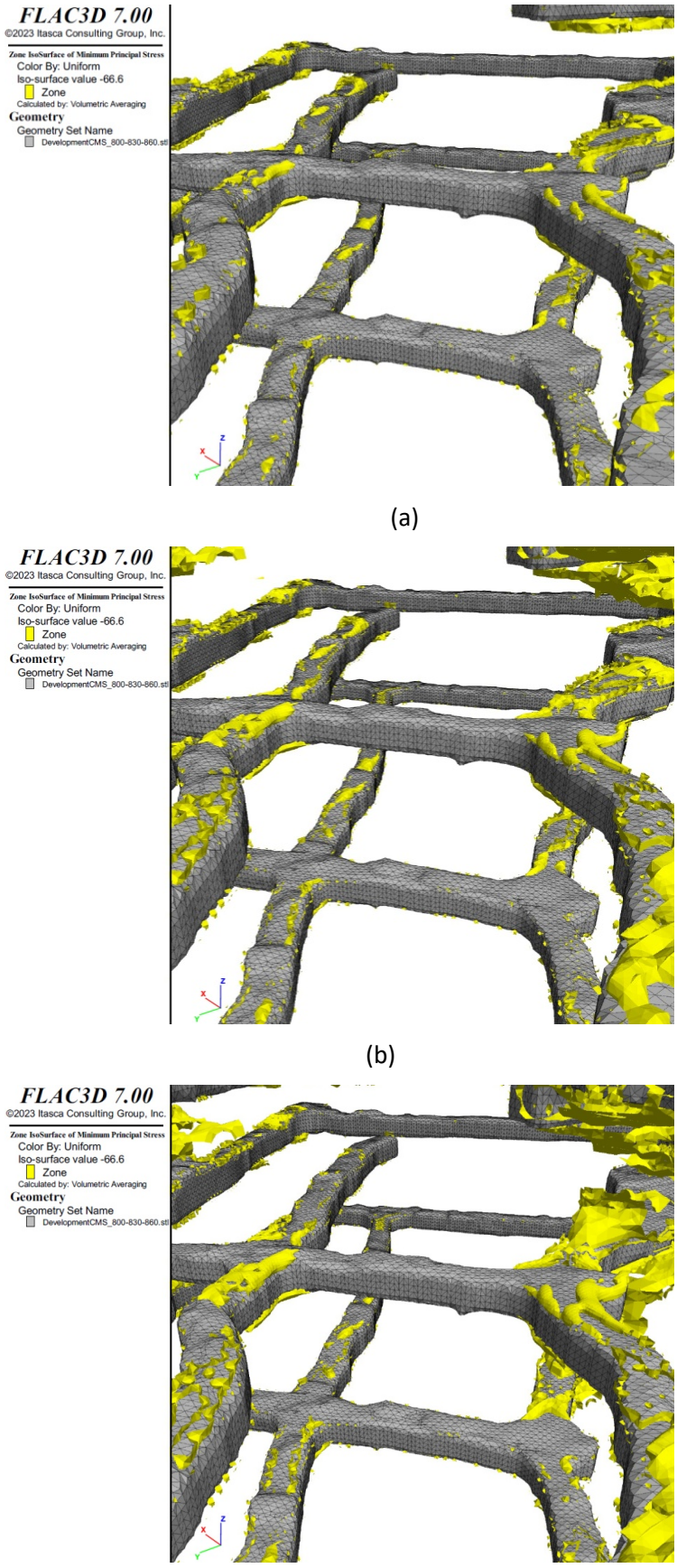

Figure 6 Major principal stress (σ_1) isosurfaces for a value of 66.6 MPa, 830/860–5050/6000-358 intersections: (a) Step 1; (b) Step 4; (c) Step 11 (final step before failure)

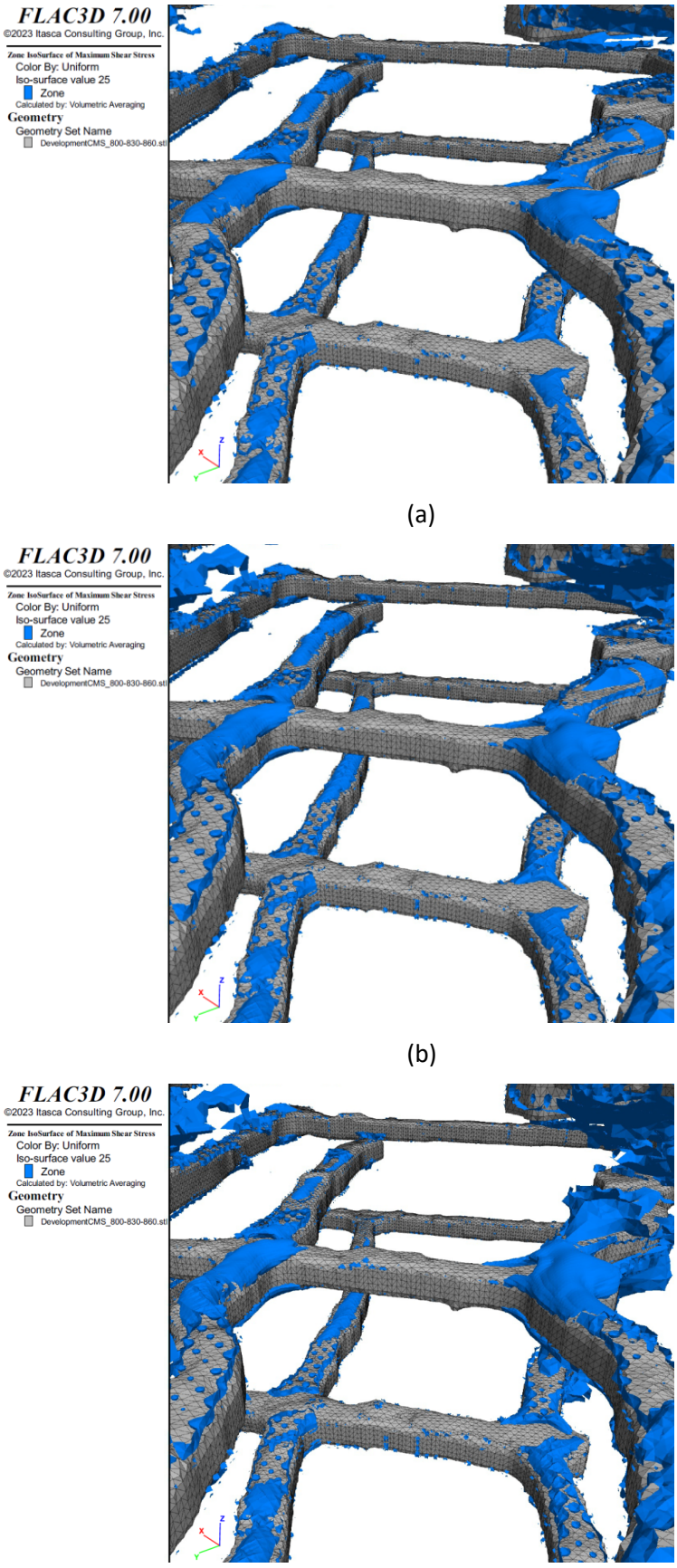

Figure 7 Maximum shear stress ($[\sigma_1-\sigma_3]/2$) isosurfaces for a value of 25 MPa, 830/860–5050/6000-358 intersections: (a) Step 1; (b) Step 4; (c) Step 11 (final step before failure)

3.3 Comparison to rock mass behaviour

The 830, 5050-358 intersection failed after step 11 with a height measured at 6.1 m, and the final cavity monitoring survey is presented in Figure 8. The detailed model confirms the concept that Kaiser et al. (1996) explain when referring to stress raisers starting at the corners of excavations and gradually forming semicircular shapes around them. The 6.1 m height does not correlate with the isosurfaces from the model, however, this can most probably be explained by the constant seismic activity which extends the depth of failure. In the model, shear stresses reach the point of potential for minor strainbursting, and the hypothesis is that minor strainbursting allows the rock mass to reach a post-peak stage, thus enabling elevated stress redistributions. The same pattern would then be repeated and a large depth of failure would be attained. On site, the east and west intersections have experienced a large number of seismic events, which might be the key to understanding such a high depth of failure.

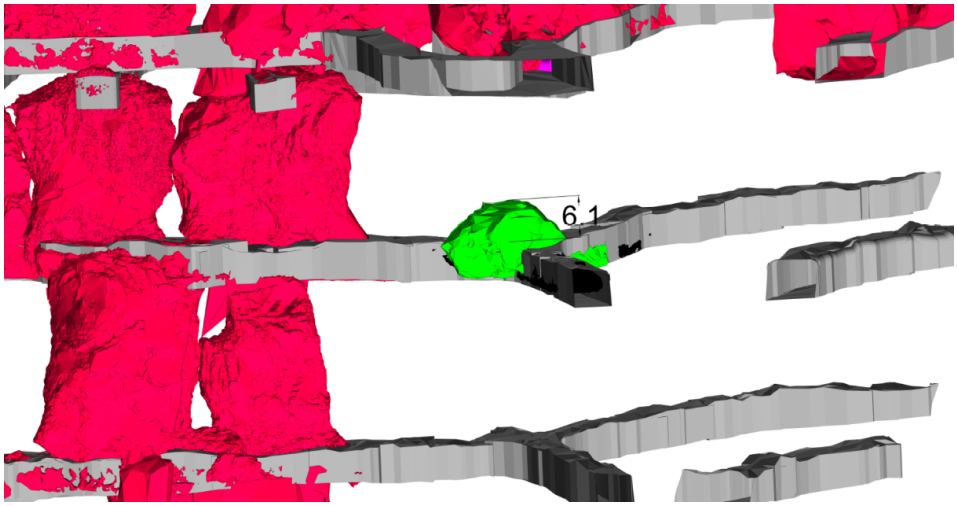

Figure 8 Cavity monitoring survey of rockfall on level 830; GMN-5050/AMN-358 intersection

3.4 Discussion

The main objective in this study was to conduct a numerical analysis for instability at key intersections at the Eleonore mine. This was attempted with a two-stage approach of using an initial geometrically simplified model to first identify sensitive locations, followed by a detailed model of these areas that could be used for an advanced analysis with different rock mass properties, in situ stress magnitudes and constitutive models. In this paper both the geometrically simplified and detailed models were run in linear elastic mode to provide maximum values of compressional and shear stresses.

Despite the use of deterministic and average rock mass properties as input parameters in both models, the geometrically simplified one was able to correctly identify intersections as sensitive areas where elevated compressive and shear stresses accumulated. In the detailed model, further information was obtained with respect to the locations (walls, floor and back) and relative volumes of unstable rock mass at these intersections. The advantage of using a combination of simplified and detailed models is that the latter type are used only in areas where potential instability is first identified, which saves considerable effort in model construction, calibration and run time. Furthermore, the detailed model can then be used with varying rock mass input parameters and constitutive models (e.g. elasto-plastic) to fine-tune its output with respect to actual field behaviour and events.

4 Conclusion

This study shows that a geometrically simplified model can help locate areas of high stress and unstable ground in a relatively rapid manner. By identifying these areas of high risk, detailed modelling can then be conducted in a method that allows a focused analysis of these regions instead of building large and time-consuming models from the start. This process was applied to the Eleonore mine and, more specifically,

to the 830 and 860 levels where intersections and drifts have experienced multiple instability events. The results showed that compressional and shear stresses were very high at the 830, 5050-358 intersection. However, by comparing the model results to real data from the mine it can be stated that the static stress is probably not the single factor responsible for such large depths of failure. In this area, dynamic stresses cannot be excluded and will also be modelled in future studies to obtain the real depth of failure.

Acknowledgement

The authors would like to acknowledge Itasca for the provision of FLAC3D licences through the Itasca Educational Partnership Teaching Program to the Department of Mining and Materials Engineering at McGill University. The authors would also like to acknowledge Cavroc for the provision of a free educational licence for StopeX.

References

Bewick, RP, Kaiser, PK & Amann, F 2019, 'Strength of massive to moderately jointed hard rock masses', *Journal of Rock Mechanics and Geotechnical Engineering*, vol. 11, no. 3, pp. 562–575, https://doi.org/10.1016/j.jrmge.2018.10.003

Bieniawski, ZT 1967, 'Mechanism of brittle fracture of rock: part III—fracture in tension and under long-term loading', *International Journal of Rock Mechanics and Mining Sciences & Geomechanics Abstracts*, vol. 4, no. 4, pp. 425–430, https://doi.org/10.1016/0148-9062(67)90032-0

Bouzeran, L, Garza-Cruz, EG & Pierce, M 2018, 'Geomechanical assessment of alternative stoping sequences at Eleonore mine', *Les Mines Opinaca Ltee*, ITASCA, Minneapolis.

Cai, M & Kaiser, PK 2014, 'In situ rock spalling strength near excavation boundaries', *Rock Mechanics and Rock Engineering*, vol. 47, pp. 659–675, https://doi.org/10.1007/s00603-013-0437-0

Cai, M, Kaiser, PK & Martin, CD 1998, 'A tensile model for the interpretation of microseismic events near underground openings', *Pure and Applied Geophysics*, vol. 153, no. 1, pp. 67–92, https://doi.org/10.1007/s000240050185

Castro, LAM, Bewick, RP & Carter, TG 2012, 'An overview of numerical modelling applied to deep mining', in L Ribeiro e Sousa (ed.), *Innovative Numerical Modelling in Geomechanics*, 1st edn, Taylor & Francis Group, London, pp. 393–414.

Cook, NGW 1983, 'Origin of rockbursts', *Proceedings Symposium on Rockbursts: Origin and Prediction*, Institution of Mining and Metallurgy, London, pp. 1–9.

Corthésy, R & Leite, MH 2017, 'Mesures des contraintes in situ mine Éléonore, rapport préliminaire', *Eleonore Mine*, Polytechnique Montréal, Bureau de la Recherche et Centre de Développement Technologique, Montreal.

Garza-Cruz, T, Bouzeran, L, Pierce, M, Jalbout, A & Ruest, M 2019, 'Evaluation of ground support design at Eleonore mine via bonded block modelling', in J Hadjigeorgiou & M Hudyma (eds), *Ground Support 2019: Proceedings of the Ninth International Symposium on Ground Support in Mining and Underground Construction*, Australian Centre for Geomechanics, Perth, pp. 341–356, https://doi.org/10.36487/ACG_rep/1925_23_Garza-Cruz

Germanovich, LN & Dyskin, AV 1988, 'A model of brittle failure for materials with cracks in uniaxial loading', *Mechanics of Solids*, vol. 23, no. 2, pp. 111–123.

Golder Associates 2009, 'Final report on geomechanical design study for the underground mine Eleonore project', *Les Mines Opinaca Ltee.*

ITASCA 2019, *FLAC3D – Fast Lagrangian Analysis of Continua in Three Dimensions*, version 7, computer software.

Kaiser, PK & Cai, M 2013, 'Critical review of design principles for rock support in burst-prone ground - time to rethink!', in Y Potvin & B Brady (eds), *Ground Support 2013: Proceedings of the Seventh International Symposium on Ground Support in Mining and Underground Construction*, Australian Centre for Geomechanics, Perth, pp. 3–37, https://doi.org/10.36487/ACG_rep/1304_01_Kaiser

Kaiser, PK, McCreath, DR & Tannant, DD 1996, *Canadian Rockburst Support Handbook*, Geomechanics Research Centre, Sudbury.

Martin, CD 1993, *The Strength of Massive Lac du Bonnet Granite Around Underground Openings*, PhD thesis, University of Manitoba, Winnipeg.

Martin, CD 1997, 'Seventeenth Canadian Geotechnical Colloquium: the effect of cohesion loss and stress path on brittle rock strength', *Canadian Geotechnical Journal*, vol. 34, no. 5, pp. 698–725, https://doi.org/10.1139/t97-030

Terrane 2019, *Report on the Structural Geology Model Update*, Éléonore Mine, paper presented at Eleonore Mine, Vancouver, November.

Vakili, A 2016, 'An improved unified constitutive model for rock material and guidelines for its application in numerical modelling', *Computers and Geotechnics*, vol. 80, pp. 261–282, https://doi.org/10.1016/j.compgeo.2016.08.020

Vakili, A, Abedian, B & Cosgriff, B 2020, 'An introduction to StopeX – a plug-in to simplify and fast-track FLAC3D numerical modelling for mining applications', in D Billaux, J Hazzard, M Nelson & M Schöpfer (eds), *Proceedings of the 5th International Itasca Symposium: Applied Numerical Modeling in Geomechanics – 2020*, Itasca International, Inc., Minneapolis, https://www.itascainternational.com/events/applied-numerical-modeling-in-geomechanics-2020

Yong, S 2014, 'In situ stress, determination, Éléonore project, Quebec', *Les Mines Opinaca Ltee*, Geomechanics Research Centre, Sudbury.